A wireless multi-channel neural amplifier for freely moving animals

Tobi A Szuts[1], Vitaliy Fadeyev[2], Sergei Kachiguine[2], Alexander Sher[2], Matthew V Grivich[2], Margarida Agrochão[3,4], Pawel Hottowy[5], Wladyslaw Dabrowski[5], Evgueniy V Lubenov[6], Athanassios G Siapas[6], Naoshige Uchida[3,7], Alan M Litke[2] & Markus Meister[3,7]

Conventional neural recording systems restrict behavioral experiments to a flat indoor environment compatible with the cable that tethers the subject to recording instruments. To overcome these constraints, we developed a wireless multi-channel system for recording neural signals from rats. The device takes up to 64 voltage signals from implanted electrodes, samples each at 20 kHz, time-division multiplexes them into one signal and transmits that output by radio frequency to a receiver up to 60 m away. The system introduces <4 μV of electrode-referred noise, comparable to wired recording systems, and outperforms existing rodent telemetry systems in channel count, weight and transmission range. This allows effective recording of brain signals in freely behaving animals. We report measurements of neural population activity taken outdoors and in tunnels. Neural firing in the visual cortex was relatively sparse, correlated even across large distances and was strongly influenced by locomotor activity.

Extracellular recording from multiple neurons in awake behaving rodents is now a common technique. Robust and lightweight drives for electrodes have been developed[1] and multiple commercial and custom-made drives are available[2]. However, the high channel count of these devices requires a multi-stranded cable to connect the headstage to the digitizing computer; this cable is easily tangled and can be heavy. As a result, the recording environment must be carefully designed to match the task. These wiring concerns constrain the range of behaviors that can be studied, particularly those that require large spaces or three dimensions, such as long-range navigation or flight. Similarly, it is difficult to explore truly natural behavior by recording brain signals in the wild.

Sensory systems respond very differently to natural stimuli than to simplified ones. Although there have been valiant attempts to design laboratory stimuli that approximate the statistical features of nature[3], these invariably miss much of the animal's experience in the wild. In the case of vision, this includes high light intensities, a large range of contrast, cues from parallax motion and integration with other brain systems in a coordinated task[4,5]. Through evolution, the brain

has adapted to interactions with the natural world and hence should transmit and process real stimuli better than artificial or simplified ones[6]. The challenge of observing neural systems during behavior in the wild can be met to a certain degree with conventional recording systems. For example, mechanized servo systems have been designed to keep the recording tether supported above a moving animal[7]. However, much greater experimental flexibility can be realized by entirely removing the wires that tether the animal to the computer.

Such a wireless design should match the channel count of existing electrode drives (50–100 channels), have a transmission distance of >20 m (longer than the longest cable systems), and be small and light enough for a rat to wear. Previous wireless devices have not met these goals; low channel count prevents recording from enough neurons to judge ensemble activity, and short transmission distance curtails the flexibility that makes wireless recording so useful in the first place. We chose the rat as the target animal because it is the most commonly used laboratory model for behavior.

The wireless device described here meets all these targets by combining three components that were originally designed for separate purposes: the tetrode microdrive, for chronic positioning of electrodes in the brain; an integrated circuit with a multi-channel amplifier/filter/multiplexer, for high channel–count neural recording[8,9]; and a radio frequency wireless transmitter, for home video surveillance systems (http://www.spystuff.com). All three components have been integrated into one system and, with custom-built software, provide a recording method that has fidelity comparable to that of rack-mounted electronics. To demonstrate the utility of this device, we made neural recordings from a premotor area and the primary visual cortex of the rat under diverse experimental conditions, including unconstrained behavior in the wild.

RESULTS
System design
The transmission system is designed to be carried by a rat. It consists of two units (head board and back board) connected by a short cable (**Fig. 1**). The head board plugs into the tetrode drive, which is implanted on the

Figure 1 System overview, showing all components (bottom left) and the complete system worn by a rat (bottom right). Roman numerals indicate points of the signal path that are illustrated in **Figure 3**. A ground shield around the outer edge of the circular headstage circuit boards (bottom left) has been removed for clarity.

rat's head, and houses the circuitry necessary to encode the transmitted signal. The back board contains the batteries, power supply circuitry and radio frequency transmitter, and is carried by a harness on the rat's back. The receiving system consists of a tunable radio frequency receiver and digitizing computer that streams the received signal directly to disk. Individual electrode voltages are extracted offline according to a reconstruction algorithm (see **Table 1** for additional physical and electrical characteristics of each component).

The tetrodes are maneuvered by a drive that is commercially available from Neuralynx, Inc. This manual, screw-based drive holds up to 28 individually adjustable probes and conveys 108 electrical channels. Our current headstage connects to 12 tetrodes and 6 single channels (54 channels in total); redesigning the connector would allow 64 channels to be processed. The drive weighs 15 g and is cemented to the animal's head during surgical implantation (**Fig. 1**). Other electrode systems can be adapted to the transmission electronics by use of an appropriately wired connector.

The head board circuit (**Fig. 2**) performs all the signal processing steps before transmission. It includes an analog readout chip to amplify, filter and multiplex the input voltages, a programmable logic chip (PLC) to supply digital control and command signals to the analog circuitry, an oscillator chip to provide the clocking signals, circuitry to generate a synchronization or calibration pulse and an output line driver. The head board is constructed as a pair of stacked interconnected round circuit boards (**Fig. 1**). The lower board contains the readout chip and connects to the tetrodes through an electrode interface board (EIB) and two multi-pin connectors. The upper board contains the PLC.

The readout chip, the core of the analog circuitry, is the 'Neuroplat' chip[10], which was designed for multi electrode array neural recording and stimulation systems[11]. This custom-designed integrated circuit contains 64 input channels with a.c. coupling, differential amplification (relative to a common reference), bandpass filtering and a simultaneous sample-and-hold circuit. The 64 output signals are interleaved onto a single output line with an analog multiplexer built into the chip.

The amplifier gain, passband frequencies and sampling rate are common to all channels and are determined by digital commands sent from the PLC to the Neuroplat chip. They can be changed by reprogramming the PLC (**Table 1**); detailed frequency characteristics have

been published previously[9]. For the experiments described below, the passband was 80–2,300 Hz, the gain was 900 and the sampling rate was 20 kHz per channel. A faster sampling rate could be programmed with a corresponding reduction in the number of channels. The line driver circuit provides an additional gain of two.

The PLC (Xilinx model #XCR3064XLP) and accessory circuits provide auxiliary functions and programmability. In addition to command signals, it supplies the Neuroplat chip with control signals for sampling, holding and multiplexing the 64 input waveforms, and for generating a synchronization or calibration pulse that marks the onset of every 64-channel scan of the Neuroplat output.

The back board carries the batteries, power-regulating circuitry and radio frequency transmitter. Two 3-V lithium batteries provide power to the transmitter, and additional voltage regulators produce duplicate ±1.6-V supplies, one for the analog circuit and one for the digital circuits. Six wires connect the back board to the head board: four voltage lines, one common ground and the multiplexed transmitter signal. The Neuroplat chip consumes 165 mW, the transmitter 200 mW, the remaining head board circuitry 100 mW and the voltage regulators 180 mW. With the current set of batteries (Sanyo CR2), which weigh 22 g, the system can operate continuously for ~6 h. With an alternate set of batteries (2L76) that weigh 7 g, the operating time is reduced to ~1 h. The battery weight prohibits placement on the head. Instead, the back board is carried by a harness, which is modified from a commercial model (Lomir RJ03). Large rats (500–600 g) can readily carry about ~10% of their body weight.

The miniaturized frequency-modulation transmitter was designed to transmit analog video signals (SpyStuff.com, Model SDX-21LP) and has not been modified. It has a bandwidth of 8 MHz, accepts an AC-coupled
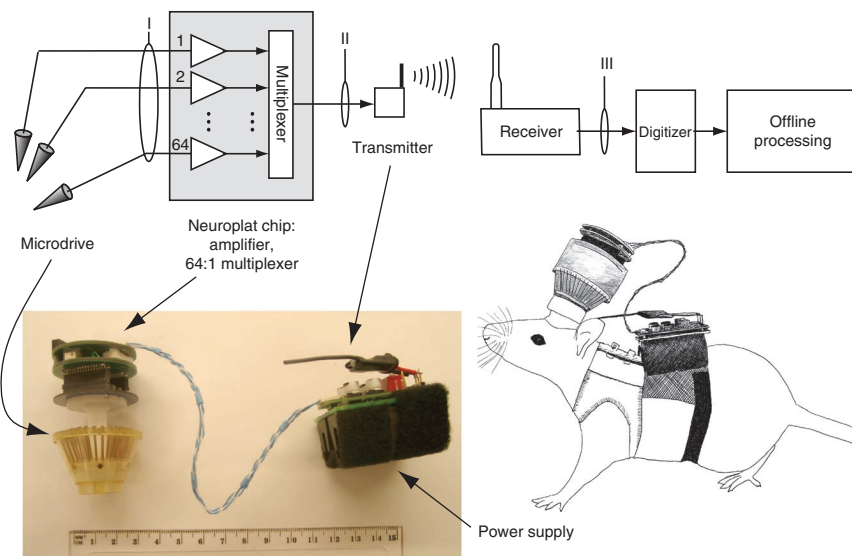
Table 1 Physical and electrical specifications of the telemetry system

Microdrive	Head board	Back board		Receiver & DAQ
		Transmitter	Power & harness	
Neuralynx 28 tetrode	64 channels	2.380 GHz	Two 3-V Li batteries	Tunable 2.2–2.5 GHz
12 tetrodes used	20 kHz per channel	Input 1 V peak-to-peak	115 mA	10 Msample per s
6 LFP channels	1,800 × gain	Range >60 m	~6 h recording	+12 dB antenna
Screw pitch 160 μm per turn	Low cutoff 10–100 Hz	Size: 5 × 1.5 × 0.3 cm	Size: 5 × 4 × 3 cm	
Size: 3.80 × 5.3 cm	High cutoff 50–4,500 Hz	Mass: 3 g	Mass: 37 g	
Mass: 15 g	Size 3.50 × 2.5 cm			
	Mass: 12 g			

Figure 2 Schematic circuits. (**a**) Block diagram of the head board: the Neuroplat chip amplifies, filters and analog multiplexes up to 64 input signals. The multiplexed signal is combined with a synchronization or calibration pulse in an analog multiplexer chip, and then buffered by a line driver. A PLC provides command and control signals to the Neuroplat chip to generate the multiplexed output and to set the channel gain and passband. The PLC also provides the control signals to the multiplexer. A 10-MHz quartz oscillator supplies the PLC's clocking signals. (**b**) Block diagram of the 64-channel Neuroplat chip[9].
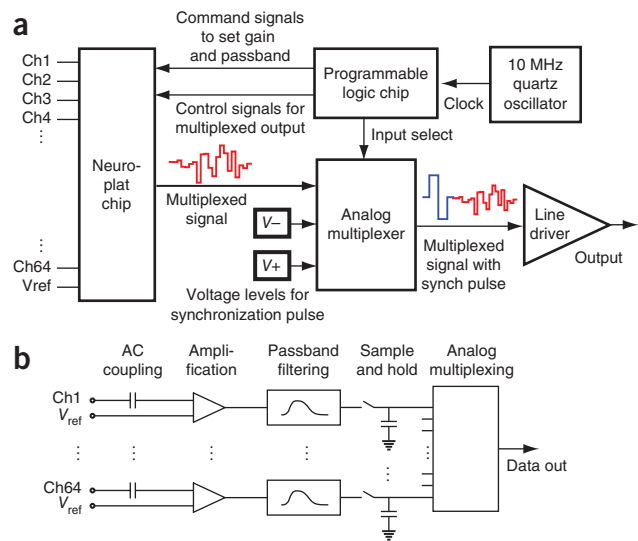
input of 1 V peak-to-peak and is powered at 6 V. Various carrier frequencies are available; our current system operates at 2.380 GHz.

The receiver was developed by the amateur television community and its circuit schematic is freely available (http://ve6atv.sbszoo.com/platinum/docs/13cmRxDwg.pdf). The receiver is tunable over the range 2.3–2.6 GHz and hence supports many different transmission frequencies. The raw demodulated output is digitized at 10 Msamples per s (National Instruments PCI-6115) and streamed directly to disk using code written in LabView.

Signal path

Figure 3 summarizes how the system encodes electrode voltages for transmission and how they are decoded after reception. Every 50 μs of input to the transmitter contains a data field that conveys one sampled voltage from each electrode. This begins with a synchronization pulse of biphasic square shape, lasting ~10 μs, and is followed by a 40-μs scan through all 64 Neuroplat channels to produce a sequence of 64 steps, each ~600 ns long (**Fig. 3**). The amplitude of each step encodes the sampled voltage. To minimize the effect of transmission noise, the transmitter includes a highpass 'pre-emphasis' filter that boosts signal power at high frequencies. This filter has a time constant of ~2 μs.

The electrode voltages are reconstructed from the received signal in three stages: convolution with a decoding filter, temporal and voltage alignment to the synchronization pulse, and linear weighting of multiple sample points for a single electrode voltage. The algorithm is currently implemented offline by code written in C and Igor (Wavemetrics).

The first stage, convolution with the decoding filter (**Fig. 3**), corrects for the pre-emphasis stage in the transmitter. This filter is essentially lowpass with additional temporal structure from the sharp transients in the Neuroplat output. The optimal filter shape was computed by comparing a test signal recorded before and after transmission.

The second stage, temporal and voltage alignment, finds each synchronization pulse and the value of its high and low phases (**Fig. 3**). Each voltage step within the data field starts at a known time offset from the synchronization pulse. The absolute voltage of the synchronization pulse is used to correct for slow baseline drift in the transmitted signal.

The third stage, linear weighting of multiple sample points, reconstructs the electrode voltage of a single channel at one time point (**Fig. 3**). As the receiver stream is digitized at 10 Msamples per s, each 600-ns voltage step is represented by 6 sample points; multiple points are averaged to reduce electronic noise. Their linear weights were chosen to minimize cross-talk between adjacent channels using a test signal with sine waves of different frequencies. Later points are weighted more heavily than earlier ones because of the settling dynamics of the analog circuit, and points close to the transition between steps are effectively ignored.

Performance

We measured the noise properties of the wireless system in a modified setup that distributed one input signal to seven Neuroplat channels. We then measured the multiplexed stream before (point II; **Fig. 1**) and after (point III) the transmitter to determine transmission fidelity (**Fig. 4**). We determined random noise from the electronics, the transmitter and the reconstruction algorithm by comparing a single instance of the electrode signal to the average of all seven nominally identical instances. We determined systematic noise from transmitter nonlinearities by comparing the average signal before and after transmission.

We converted the s.d. of noise over the band 80–2,300 Hz to equivalent electrode voltage by dividing by the system gain. Random noise from transmission was 2.80 μV root-mean-squared (r.m.s.) and systematic noise was 2.33 μV r.m.s. Added in quadrature, their sum was 3.64 μV, well below the biological noise that is inherent in extracellular recording.
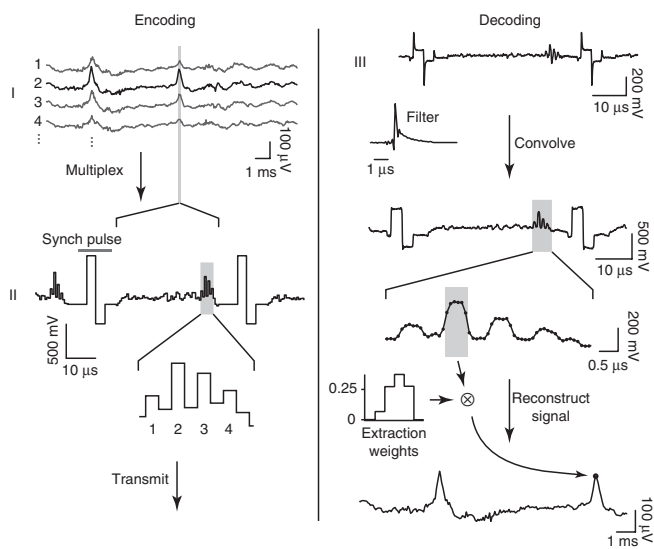
Figure 3 Signal path, showing schematically how electrode voltages are transformed by the wireless system. Raw electrode voltages (I) are first multiplexed and combined with a synchronization pulse into 50-μs data fields (II). Transmission (III) introduces a highpass pre-emphasis filter. Signal decoding follows a reverse path: first convolution with an appropriate decoding filter, then demultiplexing and reconstruction of the electrode voltage by linear weighting over the relevant data points.

Figure 4 Noise and range measurements. (**a**) Voltage trace from extracellular recording in hippocampus before and after transmission (negative voltage plotted upward). (**b,c**) Shape separation of the spikes by cluster analysis in the space of waveforms. Clusters are shown with colors: the same PCA basis was used for both. (**d**) Electrode voltages recorded at distances of 1 m and 60 m, showing spikes from two different units. Traces were bandpass filtered 500–3,000 Hz. (**e,f**) Shape separation of the spikes shown in **d**, color coded according to unit identity. The same PCA basis was used for both projections. Behavioral state was not controlled between the two conditions and probably accounts for the change in rate. (**g**) Normalized SNR as a function of transmission distance and antenna orientation, using a test signal. SNR is normalized to its value at 1 m. The receiver's stub antenna was perpendicular to the line-of-sight to the transmitter. The transmitter's antenna was either parallel to the receiver's or perpendicular, with respect to the line-of-sight path. The small dip at 30 m may derive from uncontrolled RF reflections in a cluttered environment.
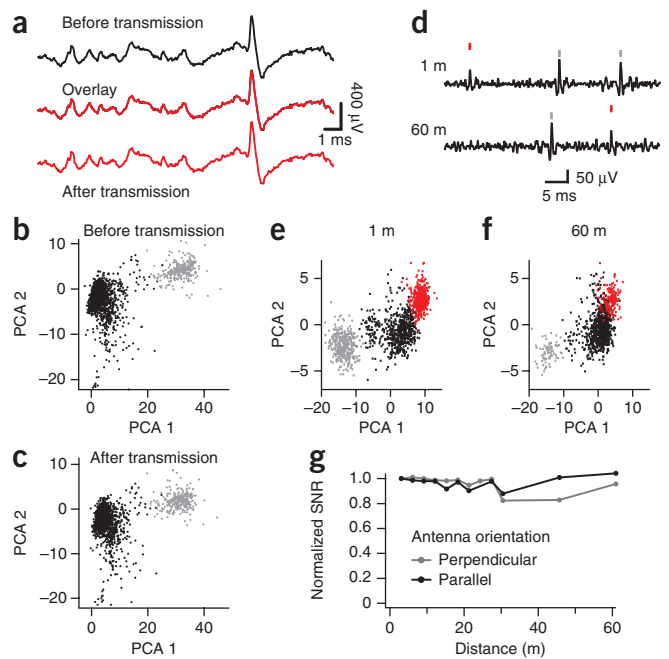
The electrode voltages that were reconstructed before and after transmission were practically identical (**Fig. 4a**): The difference between the two was considerably smaller than the background noise from neural 'hash'. To estimate the practical effects of transmission noise on spike sorting, we performed a cluster analysis of spike waveforms[12] before and after transmission (**Fig. 4b,c**). The difference in cluster shape was negligible: 2 of 213 spikes were assigned differently in the two recordings. Spike shape hardly changed with transmission distance: spikes recorded at 60 m were identical to those recorded at 1 m (**Fig. 4d**). Likewise, transmission over 60 m has little effect on cluster shape (**Fig. 4e–f**).

We measured the transmission range using a portable signal generator that produced a known and reproducible signal similar to the Neuroplat's output. The signal was a pseudo-random M-sequence, where each step lasted 1 μs, subsequent steps were chosen from 8 voltage levels and the entire sequence repeated every 0.21 s. This signal is close to the bandwidth of the Neuroplat chip output and reproduces the challenge of estimating analog voltage levels with the reconstruction algorithm (**Fig. 3**). Transmission noise was measured from the scatter of the reconstructed voltage levels about the 8 known input levels. Over a distance of 60 m, transmission quality remained high (**Fig. 4g**). Given the lack of degradation it is likely that telemetry works over an even greater range. The transmitter-receiver path in these tests was line-of-sight and the receiver used an omni-directional stub antenna. For long-distance applications, a simple directional antenna can boost signal strength by 13 dB.

To reduce interference from external radio frequency sources, the transmission frequency of 2.380 GHz was chosen because it lies outside the most crowded commercial bands (2.40–2.49 and 2.50–2.59 GHz). To measure external traffic at this frequency, we turned off the transmitter and recorded the receiver's automatic gain control level, a measure of received signal strength. In two heavily used research buildings with wireless communication systems we encountered short 1-ms pulses of interference with a power corresponding to ~30 m transmission distance, as well as very short 50 μs pulses at higher power. Neither of these signals interfered with effective data collection: transmission was disrupted <0.01% of the time. In outdoor environments the interference level can be expected to be lower still.

Cortical recordings

We have used this wireless system to record extracellular neural signals under three different conditions, listed from most constrained to least: during a behavioral task in a small cage; during free roaming in a medium-sized arena with visual stimuli; and outdoors in a field, where a wireless system is required.

To show that the new system is compatible with a motor task, we trained a rat to discriminate two odors in a behavior box[13] and implanted it with electrodes in a premotor area (sometimes called frontal eye field)[14]. After 2 d of training with the wireless system, the rat performed ~100 trials in an hour. The wireless system reliably recorded task-related firing in cortical neurons (**Fig. 5a**). In the tight geometry of this enclosure, telemetry offers the convenience of recording without a commutator and without fear that the rat might reach and damage the recording cable.

To explore visual processing under freely moving conditions, we implanted electrodes into area V1 of primary visual cortex. The rat roamed through an indoor enclosure 1 m × 1 m in size that was scattered with bedding, food rewards and nesting boxes. The animal typically spent the first 10 min exploring the arena and the remaining time sitting quietly and moving around in shorter bursts; its activity was recorded with a video camera mounted overhead. We made no attempt to control or measure eye position. However, we varied the illuminant intensity of overhead light-emitting diodes.

A periodic 4-Hz flash of the illuminant produced a clear modulation of firing in many cortical neurons, with a latency as short as 30 ms (**Fig. 5b**). The pattern of firing remained largely consistent during periods when the animal explored, even though the neurons' receptive fields must have been exposed to many different spatial patterns of visual input. During some periods when the animal rested, the kinetics of the flash response slowed markedly (**Fig. 5b**); this might reflect a gradual transition from wake to sleep states. We investigated the temporal response properties of cortical neurons further by varying the illuminant with pseudo-random binary flicker[15] (**Fig. 5c**). This revealed neurons with quite different dynamics (**Fig. 5c**). The short response latencies (~30 ms) indicate that these neurons can signal rapid events in the stimulus. Indeed, some cells fired in phase with the 20-Hz flicker rate (**Fig. 5d**). These recordings show that the system transmits reliable, stimulus-locked neural signals even under freely moving conditions, suitable to support studies of neural coding in the visual cortex.

We used the shape of the extracellular action potential to classify units into putative cellular types (**Fig. 6a**): broad spike shapes (broad spiking units, BSUs) are associated with excitatory neurons, and narrow shapes (narrow spiking units, NSUs) with inhibitory interneurons[16,17]. Altogether, 10 of 40 neurons had narrow spikes, consistent with reported

Figure 5 Illustrative data: spike trains and response properties from the rat cortex. (**a**) Activity recorded from the premotor cortex during an odor discrimination task. Raster graph shows a single-unit spike train; each row is a single trial. Spike times (black ticks) are measured relative to when the rat left the central odor delivery port ('odor port out') after odor delivery. Colored ticks indicate when a side water port was reached ('water port in') and background shading indicates which water port the animal chose. The four odorants were combinations of caproic acid (odor A) and 1-hexanol (odor B) in the ratios indicated by colored bars to the right. When odor A was stronger, the water reward came from the left port and otherwise from the right port. Below, average firing rate analyzed by response port (right versus left) and odor stimulus (indicated by color), showing response only during leftward motion. (**b**–**d**) Neurons from visual cortex recorded in an indoor arena. (**b**) Response of neuron A to the illuminant flashing periodically at 4 Hz. Top, raster graph of spikes on successive stimulus repeats. Middle, average firing rate over all repeats. Bottom, light intensity. Right, number of spikes averaged over four consecutive repeats. Far right: motion score (1 if animal moved in a given 0.5 s period, 0 otherwise). Beginning at repetitions 450 and 850, the peak latency increased gradually from 40 to 70 ms. Both changes occurred at the start of a putative sleeping period (defined by lack of motion for >15 s). (**c**) Spike-triggered average stimulus derived from the spike trains of neurons A and B under random flicker of the illuminant. Top, sample stimulus trace of 20-Hz random flicker. Bottom, average intensity (from −0.5 to 0.5) plotted as a function of time preceding an action potential. (**d**) Autocorrelation functions for neurons A and B under random flicker stimulation, colored as in **c**. The cell's average firing rate is plotted as a function of time since one of its own spikes. Neuron A was modulated at multiples of 50 ms, indicating phase-locking to the flicker rate.
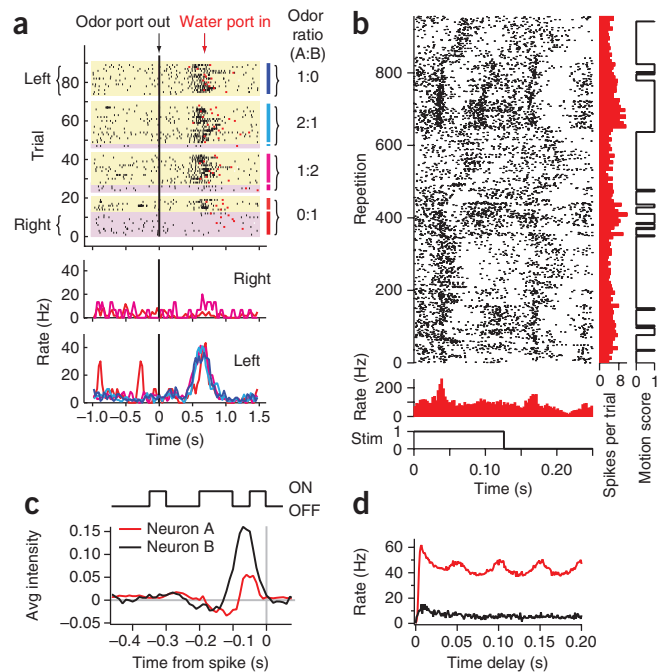
frequencies of 19–24% in mouse V1 (ref. 18). These recordings show that the sampling rate and noise levels of our system are sufficient to discriminate the spike waveforms of different neuronal types.

How the visual cortex functions in freely roaming animals is largely unexplored[19,20]. We report here some basic parameters of neural activity in rat V1. During free roaming indoors, with constant illumination, neurons fired at an average rate of 6.3 ± 8.2 Hz (mean ± s.d., range 0.1–38 Hz). These values are consistent with expectations from metabolic constraints[21] (3–5.5 Hz). In this context, it is relevant that these tetrodes were not adjusted to hunt for the most active units,

thereby avoiding a common bias in single-electrode recording. We also found that NSUs had a significantly higher average firing rate (14.3 Hz) than BSUs (3.7 Hz; $P = 0.0014$, Wilcoxon rank sum test).

The collective function of neurons in a cortical network leads to correlations in their firing on time scales from milliseconds to seconds[22]. We measured correlation functions among the spike trains of neurons during free roaming in an indoor arena under constant illumination (**Fig. 6b**). Many correlation functions showed peaks near zero delay, indicating synchronized firing, whereas dips were encountered only rarely. Most of these peaks had widths <100 ms (ref. 23). Therefore, we measured the strength of synchronized firing by a simple correlation index: the relative increase in the firing rate in the central 50-ms window around zero delay relative to the baseline rate. Over all recorded pairs, this correlation index was strongly biased to positive
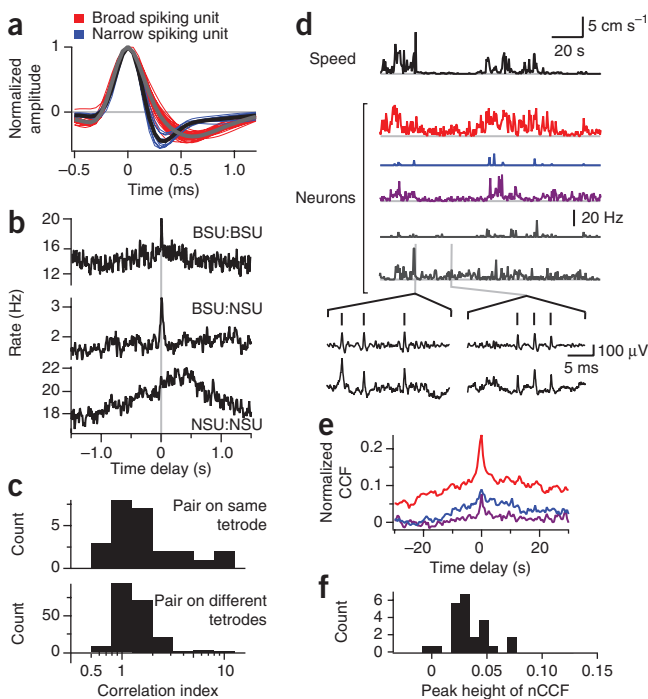
Figure 6 Population measures and behavioral modulation of V1 activity indoors. (**a**) Spike waveforms from neurons recorded in V1. The spike shapes were separated by principal component analysis (not shown) into two clusters. Bold lines are the average waveforms for the broad and narrow spike shapes. Negative voltage is plotted upwards. (**b**) Cross-correlation functions of three neuron pairs, indicating synchronized firing on different time scales. Results are plotted as the firing rate of one neuron against the delay from a spike of the other neuron. (**c**) Histogram of the correlation index for neuron pairs recorded from the same tetrode (top) and from different tetrodes (bottom). This measures the central peak of the cross-correlation function (**b**) by the ratio of the mean value in a 50-ms window around 0 s delay to the mean value around delays of 1 s and −1 s. The two distributions are not significantly different ($n = 25$ for same tetrode pairs, $n = 201$ for different; $P = 0.2$; Wilcoxon rank sum test). (**d**) Firing rate of five neurons (in 0.5-s bins, no smoothing) overlaid with the rat's speed, showing increased activity during locomotion. At the bottom, electrode traces are shown during the fastest and slowest motion episodes, to demonstrate lack of disruptive motion artifacts. The bottom trace is full bandwidth, the top trace is filtered 500–3,000 Hz. (**e**) Normalized cross-correlation functions (CCF) between neural firing rate (colored as in **a**) and the animal's speed. (**f**) Histogram of the peak height of the motion-spiking correlation function for 20 units. The peak height was measured relative to the average value at +10 and −10 s delay.
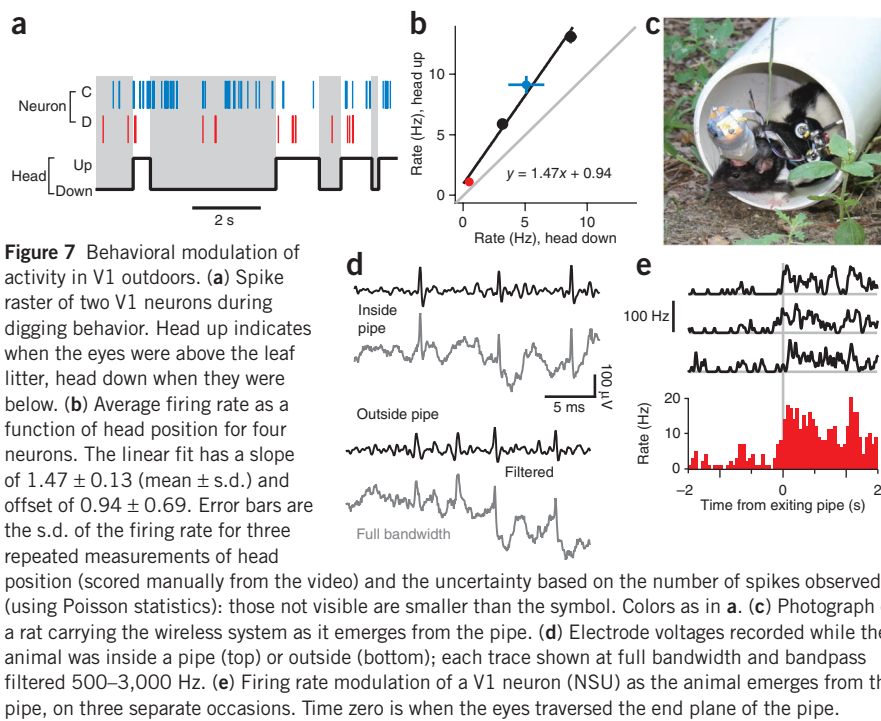
Figure 7 Behavioral modulation of activity in V1 outdoors. (**a**) Spike raster of two V1 neurons during digging behavior. Head up indicates when the eyes were above the leaf litter, head down when they were below. (**b**) Average firing rate as a function of head position for four neurons. The linear fit has a slope of 1.47 ± 0.13 (mean ± s.d.) and offset of 0.94 ± 0.69. Error bars are the s.d. of the firing rate for three repeated measurements of head position (scored manually from the video) and the uncertainty based on the number of spikes observed (using Poisson statistics): those not visible are smaller than the symbol. Colors as in **a**. (**c**) Photograph of a rat carrying the wireless system as it emerges from the pipe. (**d**) Electrode voltages recorded while the animal was inside a pipe (top) or outside (bottom); each trace shown at full bandwidth and bandpass filtered 500–3,000 Hz. (**e**) Firing rate modulation of a V1 neuron (NSU) as the animal emerges from the pipe, on three separate occasions. Time zero is when the eyes traversed the end plane of the pipe.

values (**Fig. 6c**). Correlations were of similar strength for neuron pairs recorded on the same tetrode (within a radius of 65 μm or less[24]) as for pairs from different tetrodes, spaced up to 1 mm apart (**Fig. 6c**). This indicates that concerted firing extends over large distances during free behavior. Such patterns may be caused by stimulus correlations, such as power-law correlations in natural scenes or optic flow from the animal's movements, or by long-range cortical networks.

To explore this question further, we compared the firing of V1 neurons with the rat's locomotor activity (**Fig. 6d**). Correlation functions between body speed and neural firing systematically showed peaks near zero delay with a width of 1–2 s (**Fig. 6e,f**, 23 of 24 neurons, no difference between BSUs and NSUs). This influence might derive from the global optic flow of the visual image on the retina. Alternatively, such effects could be caused by top-down influences from other brain areas[25].

Finally, we investigated activity in visual cortex when the rat moved freely in the wild. These recordings were performed during daytime in an open field ~10 m in size. The area was adjacent to woods and contained plant ground cover, dead leaves, twigs, a dead tree and solid walls. In each 60-min session, the animal was constantly engaged with its environment: it explored both the edges and the interior, dug through the leaf pile and built a nest. Neural signals were recorded from V1 and behavior was monitored with a video camera.

For four illustrative BSUs recorded on a single tetrode the average firing rates ranged from 1 to 10 Hz (**Fig. 7a,b**). All four neurons were modulated by nest-building behavior. For example, during 91 s of nest-building activity, the average firing rate was $47 \pm 13\%$ (mean ± s.d.) higher when the head was above the leaf litter (for 53 s) than when the head was below (for 38 s; **Fig. 7a,b**). All neurons showed a significant rate change between these two conditions (**Fig. 7b**; $P < 0.01$, linear regression), perhaps due to the resulting luminance differences.

To mimic rat burrows in natural habitats[26], we introduced a plastic pipe into the arena (**Fig. 7c**). Burrowing behavior requires wireless recording; as PVC is transparent to radio frequency signals, signal quality

in the pipe was unaffected (**Fig. 7d**). One of the neurons recorded showed a systematic and large rate increase lasting <2 s whenever the animal left the pipe (**Fig. 7e**). Again, these strong responses are probably driven by changes in visual input as the animal moves.

In summary, these results show the viability of recording neural signals from the rat cortex during complex and previously uncharacterized behavior both indoors and outdoors. It is notable how much of V1 firing seems to be driven by the rat's locomotor behavior. These early observations underline the need to consider visual processing in the full context of coordinated behaviors.

DISCUSSION

In recent years there has been great interest in wireless telemetry of brain signals, and efforts have focused primarily on two target applications: human brain implants that transmit across the skull and skin for clinical use[27,28], and devices carried by freely moving small animals for basic research into brain function[29–31]. The brain implant needs to transmit over a short distance but is subject to severe constraints on heat dissipation and power usage. For a small-animal system, a large transmission range is desirable, but it must meet tight weight limits to allow natural behaviors. In addition, an effective assessment of neural population codes requires a large channel count.

Among the small-animal systems reported recently (**Supplementary Table 1**), two are notable for their performance. One 16-channel device transmits pre-processed spikes over 30 m, although no test of signal quality was reported to document that range[30]. Another system meant for primates transmits 32 channels over 20 m but remains too heavy for a rat[32,33]. Several other devices are limited by a transmission range less than 5 m (ref. 31); this confines the animal to a small arena, a situation in which wired recording has already been successful. Overall, the system described here exceeds the performance of all other small-animal devices and makes it possible to record from many neurons in a large outdoor environment. Indeed, outdoor population recordings are presented here for the first time, to our knowledge.

To achieve the large range, we allocated almost one-third of the power budget to the transmitter, a component that was originally designed to transmit video over 300 m. In turn, this influenced the design decision between analog and digital transmission. The advantages of analog transmission are simplicity and low power use for a given range. Advantages of digital transmission include robustness to noise, flexible transmission protocols and signal processing techniques for data compression. Such systems often require power-hungry computing on board the animal, and robust transmission comes at the cost of lower bandwidth. For example, an alternative small-animal system using Bluetooth transmission[30] had a total data rate of 115 kbps, about 100-fold lower than for our device. Given those constraints, the headstage transmits only the 1% of data that exceed a preset voltage threshold. This prevents the use of more sophisticated offline spike sorting methods that use subthreshold signals on many channels, or the analysis of slow field potentials. Another system for macaque monkeys uses digital transmission to sustain data rates of 24 Mbps, twice as fast as ours[33]. That data rate is achieved by a custom packet structure with minimal overhead and a judicious low-power

design, at the cost of a somewhat shorter range (20 m). In summary, the current tradeoffs between analog and digital transmission are roughly equal, but as digital transmitters become smaller, cheaper and less power-hungry, this balance may shift in the future.

Several technical improvements will further enhance the utility of this device. A fast reconstruction algorithm that can decode the wireless signal and display spikes in real time will help to provide immediate feedback, in particular when adjusting tetrode depth. On the headstage, a simple infrared switch that powered the system on or off would conserve power between recording sessions without disturbing the animal. A more substantial redesign of the Neuroplat chip would also allow signal frequencies <10 Hz to be recorded, such as theta-range local field potentials or breathing rhythms. One can contemplate further miniaturization for applications to the mouse, an experimental animal that is increasingly popular in brain science[34]. Miniaturized electrode drives have been built, but their weight needs to be supported by a servo system[35] or a helium balloon[36]. To allow truly unconstrained movement of the mouse, a wireless system should not exceed ~5 g in total weight, which is about tenfold less than our current system with the lightest batteries. Thus an adaptation to the mouse would require substantial redesign and compromises on channel count, recording time or transmission distance.

However, for rat-sized animals the present wireless device rivals in all performance parameters the commercially available wired systems. As shown here, the system already supports novel scientific experiments. Eventually, this or similar instruments will see widespread use in neurophysiology laboratories and replace bulky, expensive amplifier racks. In applications where the harness and backpack are undesirable, the headstage can be used by itself in a minimally wired configuration (6 wires instead of >65 for a conventional headstage). But in wireless mode, the system removes all the experimental and geometric constraints of conventional recording technology. Neural recording is now possible in the wild and in three-dimensional environments such as tunnels. This opens the door to ecologically correct studies of brain processes during natural behaviors: visual orientation, long-range navigation or even auditory localization of a flying owl's prey.

METHODS

Methods and any associated references are available in the online version of the paper at http://www.nature.com/natureneuroscience/.

Note: Supplementary information is available on the Nature Neuroscience website.

AUTHOR CONTRIBUTIONS
This manuscript was written by T.A.S. and M.M., with comments from all authors. The Neuroplat chip was designed by P.H., W.D. and A.M.L. The back and head boards were designed by A.M.L., V.F., S.K., A.S. and M.V.G. The wireless link was designed by T.A.S. and M.M. Implantations and experiments were performed by A.G.S. and E.V.L. (hippocampus), N.U. (frontal eye field), and T.A.S. and M.A. (V1). Analysis was performed by N.U. (FEF) and T.A.S. and M.M. (V1, hippocampus). M.M. and A.M.L. supervised the project.

COMPETING FINANCIAL INTERESTS
The authors declare no competing financial interests.

1. Wilson, M.A. & McNaughton, B.L. Dynamics of the hippocampal ensemble code for space. *Science* **261**, 1055–1058 (1993).
2. Jog, M.S. *et al.* Tetrode technology: advances in implantable hardware, neuroimaging, and data analysis techniques. *J. Neurosci. Methods* **117**, 141–152 (2002).
3. Felsen, G. & Dan, Y. A natural approach to studying vision. *Nat. Neurosci.* **8**, 1643–1646 (2005).
4. Lewen, G.D., Bialek, W. & de Ruyter van Steveninck, R.R. Neural coding of naturalistic motion stimuli. *Network* **12**, 317–329 (2001).
5. Reppas, J.B., Usrey, W.M. & Reid, R.C. Saccadic eye movements modulate visual responses in the lateral geniculate nucleus. *Neuron* **35**, 961–974 (2002).
6. Barlow, H.B. in *Sensory Communication* (ed. Rosenblith, W.A.) 217–234 (MIT Press, Cambridge, Massachusetts, 1961).
7. Brun, V.H. *et al.* Progressive increase in grid scale from dorsal to ventral medial entorhinal cortex. *Hippocampus* **18**, 1200–1212 (2008).
8. Dabrowski, W. *et al.* Development of front-end ASICs for imaging neuronal activity in live tissue. *Nucl. Instrum. Methods Phys. Res. A* **541**, 405–411 (2005).
9. Dabrowski, W., Grybos, P. & Litke, A.M. A low noise multichannel integrated circuit for recording neuronal signals using microelectrode arrays. *Biosens. Bioelectron.* **19**, 749–761 (2004).
10. Grybos, P., Dabrowski, W., Hottowy, P., Fiutowski, T. & Bielewicz, B. Neuroplat64 – low noise CMOS integrated circuit for neural recording applications. *Proc. 5th Int. Meet. Substrate-integrated Micro Electrode Arrays*, 208–209 (2006).
11. Hottowy, P. *et al.* An MEA-based system for multichannel, low artifact stimulation and recording of neural activity. *Proc. 6th Int. Meet. Substrate-integrated Micro Electrode Arrays*, 261–265 (2008).
12. Pouzat, C., Mazor, O. & Laurent, G. Using noise signature to optimize spike-sorting and to assess neuronal classification quality. *J. Neurosci. Methods* **122**, 43–57 (2002).
13. Uchida, N. & Mainen, Z.F. Speed and accuracy of olfactory discrimination in the rat. *Nat. Neurosci.* **6**, 1224–1229 (2003).
14. Sinnamon, H.M. & Galer, B.S. Head movements elicited by electrical stimulation of the anteromedial cortex of the rat. *Physiol. Behav.* **33**, 185–190 (1984).
15. Reid, R.C., Victor, J.D. & Shapley, R.M. The use of m-sequences in the analysis of visual neurons: linear receptive field properties. *Vis. Neurosci.* **14**, 1015–1027 (1997).
16. Barthó, P. *et al.* Characterization of neocortical principal cells and interneurons by network interactions and extracellular features. *J. Neurophysiol.* **92**, 600–608 (2004).
17. McCormick, D.A., Connors, B.W., Lighthall, J.W. & Prince, D.A. Comparative electrophysiology of pyramidal and sparsely spiny stellate neurons of the neocortex. *J. Neurophysiol.* **54**, 782–806 (1985).
18. Niell, C.M. & Stryker, M.P. Highly selective receptive fields in mouse visual cortex. *J. Neurosci.* **28**, 7520–7536 (2008).
19. Ji, D. & Wilson, M.A. Coordinated memory replay in the visual cortex and hippocampus during sleep. *Nat. Neurosci.* **10**, 100–107 (2007).
20. Sawinski, J. *et al.* Visually evoked activity in cortical cells imaged in freely moving animals. *Proc. Natl. Acad. Sci. USA* **106**, 19557–19562 (2009).
21. Laughlin, S.B. & Sejnowski, T.J. Communication in neuronal networks. *Science* **301**, 1870–1874 (2003).
22. Kohn, A., Zandvakili, A. & Smith, M.A. Correlations and brain states: from electrophysiology to functional imaging. *Curr. Opin. Neurobiol.* **19**, 434–438 (2009).
23. Jermakowicz, W.J., Chen, X., Khaytin, I., Bonds, A.B. & Casagrande, V.A. Relationship between spontaneous and evoked spike-time correlations in primate visual cortex. *J. Neurophysiol.* **101**, 2279–2289 (2009).
24. Gray, C.M., Maldonado, P.E., Wilson, M. & McNaughton, B. Tetrodes markedly improve the reliability and yield of multiple single-unit isolation from multi-unit recordings in cat striate cortex. *J. Neurosci. Methods* **63**, 43–54 (1995).
25. Niell, C.M. & Stryker, M.P. Modulation of visual responses by behavioral state in mouse visual cortex. *Neuron* **65**, 472–479 (2010).
26. Calhoun, J.B. *The Ecology and Sociology of the Norway Rat* (U.S. Dept. of Health, Education, and Welfare, Public Health Service, Bethesda, Maryland, 1963).
27. Borton, D.A. *et al.* Wireless, high-bandwidth recordings from non-human primate motor cortex using a scalable 16-Ch implantable microsystem. *Conf. Proc. IEEE Eng. Med. Biol. Soc.* **2009**, 5531–5534 (2009).
28. Harrison, R.R. *et al.* Wireless neural recording with single low-power integrated circuit. *IEEE Trans. Neural Syst. Rehabil. Eng.* **17**, 322–329 (2009).
29. Gregory, J.A. *et al.* Low-cost wireless neural recording system and software. *Conf. Proc. IEEE Eng. Med. Biol. Soc.* **2009**, 3833–3836 (2009).
30. Hampson, R.E., Collins, V. & Deadwyler, S.A. A wireless recording system that utilizes Bluetooth technology to transmit neural activity in freely moving animals. *J. Neurosci. Methods* **182**, 195–204 (2009).
31. Yin, M., Lee, S.B. & Ghovanloo, M. *In vivo* testing of a low noise 32-channel wireless neural recording system. *Conf. Proc. IEEE Eng. Med. Biol. Soc.* **2009**, 1608–1611 (2009).
32. Chestek, C.A. *et al.* HermesC: low-power wireless neural recording system for freely moving primates. *IEEE Trans. Neural Syst. Rehabil. Eng.* **17**, 330–338 (2009).
33. Miranda, H. *et al.* A high-rate long-range wireless transmission system for simultaneous multichannel neural recording applications. *IEEE Trans. Biomed. Circ. Syst.* **4**, 181–191 (2010).
34. Chalupa, L.M. & Willams, R.W. *Eye, Retina, and Visual System of the Mouse* (MIT Press, Cambridge, Massachusetts, 2008).
35. Yamamoto, J. & Wilson, M.A. Large-scale chronically implantable precision motorized microdrive array for freely behaving animals. *J. Neurophysiol.* **100**, 2430–2440 (2008).
36. Lin, L. *et al.* Large-scale neural ensemble recording in the brains of freely behaving mice. *J. Neurosci. Methods* **155**, 28–38 (2006).

ONLINE METHODS

Surgical procedures. Long Evans rats (male, 500–700 g, 2+ months old) were obtained from Charles River Laboratories. Anesthesia was induced with isoflurane and maintained either by intraperitoneal injections of ketamine (60 mg kg^{-1}) and medetomidine (0.5 mg kg^{-1}) or with isoflurane (1.5%–2% in O$_2$). The dorsal surface of the skull was cleaned of soft tissue and seven anchor screws were attached to the bone. A small hole (1–2 mm wide) was drilled above the implantation site and the bone and dura were removed. The location of the craniotomy was: for the frontal eye field region, +1.4 mm posterior from Bregma (AP), 1.5 mm to the right of the midline (ML); for visual cortex, +7.1 mm AP, 3.1 mm ML; and for the dorsal hippocampus, +3.8 mm AP, 2.5 mm ML. Once the electrode drive was lowered into place, the surface of the brain was protected with Vaseline and the tip of the drive was attached to the skull with a cone of dental acrylic. Recovery lasted 3 days, during which time ketoprofen analgesic (1.3 mg kg^{-1}) was given. Five rats had V1 implantations and one rat was used for each other location. All animal procedures were approved by the Institutional Animal Care and Use Committees at Harvard (visual cortex and frontal eye field) and at Caltech (hippocampus).

Behavioral training. The animal with the frontal eye field implantation was trained in an odor discrimination task[13]. Briefly, the animal learned to associate multiple odorants with the location of a water reward. The odorant was delivered at saturating vapor pressure to a central nose-poke port; water was available from a small tube in either the left or right water port, depending on the odor. Infrared beams in each port monitored when the animal entered and exited; the odor was presented with a variable delay after a central nose poke. To increase motivation, the subject had access to water only in the context of the behavioral task and for 30 min afterward.

Recording conditions. Tetrode recordings were conducted as described[37,38]: In brief, tetrodes were lowered slowly over days to their target layer and adjusted by <100 μm each day until neural signals were found. While searching for cells, a wired recording system from Neuralynx (Cheetah System) or a modified version of this system was used for real-time feedback on spike shape and statistics. The modified wired version uses timing information from the head board to trigger acquisition, and therefore bypasses the wireless reconstruction algorithm. Once neurons were present, the back board was attached to the harness and connected to the head board. Spike sorting was performed offline with a custom supervised sorting algorithm[12].

Freely roaming experiments took place within a 1 m × 1 m arena in the laboratory, illuminated by white overhead light-emitting diodes and red light for video recording. In three animals on 6 recording days, 46 units were found. Motion was scored in two ways: (i) the location of a reference point above the rat's shoulders was manually tracked every 0.5 s to determine body location and velocity; and (ii) a binary score indicating motion or no motion was computed at the frame rate of 30 Hz. The second score was more appropriate during sessile periods.

Outdoor recordings took place at the Concord Field Station, in a fenced 10 m × 10 m enclosure. Six units and video were recorded during two 60-min recording sessions with two animals. The distance between the animal and the receiver varied from 1 m to 10 m. Head position was scored manually for each frame of the video recording, indicating head above or below the leaves, or head inside or outside the end of the pipe, and repeated three times. Uncertainties quoted for firing rates (**Fig. 7b**) include both the experimental variability in scoring head position and the uncertainty from finite spike counts. The significance of rate differences was assessed with a one-tailed Z-test.

37. Feierstein, C.E., Quirk, M.C., Uchida, N., Sosulski, D.L. & Mainen, Z.F. Representation of spatial goals in rat orbitofrontal cortex. *Neuron* **51**, 495–507 (2006).
38. Siapas, A.G., Lubenov, E.V. & Wilson, M.A. Prefrontal phase locking to hippocampal theta oscillations. *Neuron* **46**, 141–151 (2005).